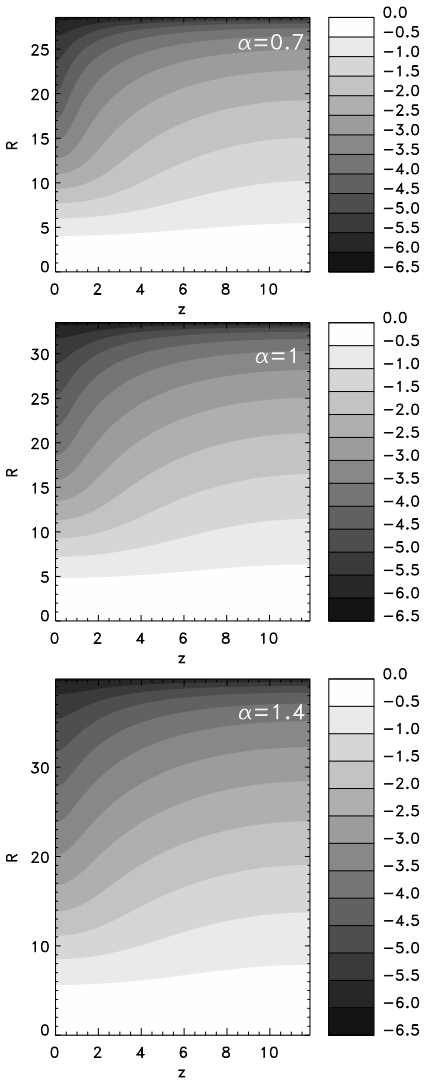

Fig. 5. Grayscale map of the magnetic flux $\Phi(z, R)$ in a natural logarithmic scale for the final state for $\lambda_z/2 = 12$ (in dimensionless units) and different values of α. The radial gravitational acceleration g_R was assumed to be constant.

$q(A)$ and $q(\Phi)$ should not lead us to the false conclusion that the source terms of the elliptic differential equations, namely $Q_{xy}(x, y)$ and $Q_{zR}(z, R)$, are also similar. Figure 4 displays Q_{xy} at two different cuts along $x = 0$ and $x = X_{\max}$, and Q_{zR} along $z = 0$ and $z = Z_{\max}$. The fractional change of Q_{xy} from its initial value is always larger than the change of Q_{zR}. Both Q_{xy} and Q_{zR} may present two local maxima along a cut through the maximum heights of the magnetic field lines, i.e., along $x = X_{\max}$ and $z = Z_{\max}$. The relative amplitude of these maxima varies with the wavelength of the perturbation.

Figure 5 shows contour plots of the magnetic flux in the final axisymmetric state for a disturbance with $\lambda_z/2 = 12$ and three different α values ($\alpha = 0.7, 1.0$ and 1.4). We see that the maps are a scaled version of each other by the factor $1+\alpha$. Since it is common for astrophysical purposes to assume equipartition between magnetic field and gas pressures, we will restrict ourselves to the case $\alpha = 1$ hereafter.

Figure 6 exhibits contour plots of the density (grayscale image) and magnetic field lines in the final stable state of the axisymmetric model for three different horizontal wavelengths ($\lambda_z/2 = 9, 12$ and 24). For comparison, density and magnetic field lines are also shown for the Cartesian model. Although the vertical size of the computational domain is larger in the axisymmetric case, we show the same box in all the cases for ease in visualization. When the systems are disturbed with the same wavelength, it is clear from Figure 6 that the field lines and the density contours become more deformed in the Cartesian model than under axial symmetry. It turns out that a cylindrical initial configuration is more rigid to perturbations and the magnetic field is less buoyant than a plane-parallel layer. Interestingly, the same degree of deformation of magnetic field lines found for $\lambda_x/2 = 9$ in the Cartesian model, can be achieved in the axisymmetric case but for a longer wavelength of $\lambda_z/2 = 12$. Likewise, the level of radial buoyancy of the magnetic field for $\lambda_z/2 = 15$ is comparable to the level of vertical buoyancy for $\lambda_x/2 = 12$ in the Cartesian model.

The column density map of a filament with $\alpha = 1$ and whose axis of symmetry lies in the plane of the sky is given in Figure 7 in the initial and final equilibrium states with $\lambda_z/2 = 15$. The scaleheight of the column density along a condensation in the direction perperdicular to z is about twice the scaleheight in the wings of the condensations. As a consequence of the less efficient drainage of gas into the magnetic valleys, the column density enhancement in the gas condensations is rather modest. In fact, the maximum enhancement in the column density over a line of sight with zero impact parameter is smaller than in the Cartesian model (see Figure 8). The column density may increase up to a factor of 7/4 in Cartesian geometry (see also Kim, Ryu, & Hong 2004) but only by a factor of 5/4 in the axisymmetric model.

The result that a cylindrical configuration is more rigid than a plane-parallel layer has, *a posteriori*, a simple geometrical explanation, as follows. Since magnetic forces act only perpendicular to the field lines, gas pressure gradients must balance the gravitational forces along a field line regardless the ge-